

Fluid description of the cooperative scattering of light by spherical atomic clouds

N. PIOVELLA¹, R. BACHELARD² and PH. W. COURTEILLE²

¹Dipartimento di Fisica, Università degli Studi di Milano, Via Celoria 16, Milano I-20133, Italy
(nicola.piovella@unimi.it)

²Instituto de Física de São Carlos, Universidade de São Paulo, 13560-970 São Carlos, SP, Brazil

(Received 15 December 2012; revised 8 February 2013; accepted 11 February 2013; first published online 14 March 2013)

Abstract. When a cold atomic gas is illuminated by a quasi-resonant laser beam, light-induced dipole–dipole correlations make the scattering of light a cooperative process. Once a fluid description is adopted for the atoms, many scattering properties are captured by the definition of a complex refractive index. The solution of the scattering problem is here presented for spherical atomic clouds of arbitrary density profiles, such as parabolic densities characteristic of ultra-cold clouds. A new solution for clouds with infinite boundaries is derived, which is particularly useful for the Gaussian densities of thermal atomic clouds. The presence of Mie resonances, a signature of the cloud acting as a cavity for the light, is discussed. These resonances leave their fingerprint in various observables such as the scattered intensity or in the radiation pressure force, and can be observed by tuning the frequency of the incident laser field or the atom number.

1. Introduction

Ultra-cold and quantum plasmas have shown an increasing interest for their analogies with cold atomic systems (Mendonça et al. 2008; Mendonça and Terças 2013). In the dilute regime, direct particle interactions can often be neglected and the particles are interacting only via their common radiation field. Furthermore, cold atomic systems are often at the borderline between classical and quantum realms, allowing to investigate in a controlled way how cooperativity changes when a transition to a quantum regime occurs. A simple example is provided by a cold atomic cloud released from a magneto-optical trap and illuminated by a laser beam (Bender et al. 2010; Bienaimé et al. 2010). Such a system manifests many interesting effects when the atomic cloud loses its granularity and can be described as a continuous fluid (Prasad and Glauber 2010). As size, shape and density of the scatterer vary, a variety of radiating patterns emerge, well known since the pioneering studies of Mie on extended dielectric particles (Mie 1908; van de Hulst 1981).

Although Mie scattering from a uniform dielectric sphere already represents a rather complex problem, light scattering by cold atoms adds new features that deserve dedicated studies (Bachelard et al. 2011, 2012b). First, changing the laser wavelength allows us to tune the light–matter interaction: this allowed to observe experimentally the transition from single-atom scattering to Mie scattering by a macroscopic object, when the collective effects appear (Bender et al. 2010; Courteille et al. 2010). Second, the weakness of direct inter-particle interactions allows us to probe the forces that light exerts on

each individual atom: in particular, for ultra-cold atomic clouds the pattern of atomic recoil was shown to contain the history of the interaction, and to exhibit signatures of anisotropy of the Mie scattering (Bachelard et al. 2012a). Finally, various geometries, atomic densities and ordered or disordered structures can be generated by designing appropriate magnetic and optical traps for the atoms. This illustrates the flexibility of cold atom experiments to model and investigate phenomena from various fields, such as condensed matter and possibly plasmas.

In this paper, we present the solution of the Mie scalar scattering problem for spherical inhomogeneous atomic clouds, with finite and infinite boundary conditions. Beyond the classical Mie solution for hard and homogeneous dielectric spheres, it provides a realistic description of light scattering by dilute atomic clouds. We discuss the possibility for the cloud to act as a resonant cavity for the light, and the signatures of this behavior.

2. The scattering equation

Let us consider a sample of N cold two-level atoms with resonant frequency ω_a , line width $\Gamma = d^2\omega_a^3/2\pi\hbar\epsilon_0c^3$ and electric dipole transition matrix element d . When illuminated by a uniform laser beam with electric field amplitude E_0 , frequency ω_0 and wave vector $\mathbf{k}_0 = (\omega_0/c)\hat{\mathbf{e}}_z$, their response is described for weak incident fields by the following coupled equations (Scully et al. 2006; Svidzinsky et al. 2008, 2010; Courteille et al.

2010):

$$\frac{\partial \beta_j}{\partial t} = i\Delta_0 \beta_j(t) - i \frac{dE_0}{2\hbar} e^{ik_0 \cdot \mathbf{r}_j} - \frac{\Gamma}{2} \sum_{m=1}^N \frac{\exp(ik_0 |\mathbf{r}_j - \mathbf{r}_m|)}{ik_0 |\mathbf{r}_j - \mathbf{r}_m|} \beta_m(t), \quad (2.1)$$

with $\Delta_0 = \omega_0 - \omega_a$, \mathbf{r}_j being the position of atom j , and β_j its complex probability amplitude to be excited at time t . The scattering kernel

$$G(\mathbf{r}, \mathbf{r}') = \frac{\exp(ik_0 |\mathbf{r} - \mathbf{r}'|)}{ik_0 |\mathbf{r} - \mathbf{r}'|} \quad (2.2)$$

has a real component that describes the *collective* (superradiant) atomic decay (Svidzinsky et al. 2008), and an imaginary component that contains the collective Lamb shift due to a light-induced short-range interaction between the atoms (Friedberg et al. 1973; Scully and Svidzinsky 2009, 2010). The latter becomes significant when the number of atoms in a cubic optical wavelength, $\rho \lambda^3$, is larger than unity. Equation (2.1) has been obtained assuming that at most one atom is excited (Scully et al. 2006; Courteille et al. 2010). However, this model has also been shown to describe the dynamics of coupled classical linear oscillators (Svidzinsky et al. 2010), so that the many-body features of cooperative scattering by two-level atoms may be understood as a classical effect. Note that this analogy holds only in the weak excitation limit of the atomic ensemble. Furthermore, in this approach short-range dipole interactions and polarization effects are neglected (Friedberg et al. 1973).

Neglecting granularity and isolating the self-decaying term $-(\Gamma/2)\beta_j$, (2.1) takes the form of an integro-differential fluid equation for the complex field $\beta(\mathbf{r}, t)$ (Bachelard et al. 2012b):

$$\frac{\partial \beta(\mathbf{r}, t)}{\partial t} = \left(i\Delta_0 - \frac{\Gamma}{2} \right) \beta(\mathbf{r}, t) - i \frac{dE_0}{2\hbar} e^{ik_0 \cdot \mathbf{r}} - \frac{\Gamma}{2} \int d\mathbf{r}' \rho(\mathbf{r}') G(\mathbf{r}, \mathbf{r}') \beta(\mathbf{r}', t), \quad (2.3)$$

where $\rho(\mathbf{r})$ is the atomic density. At a steady state, (2.3) yields

$$\int d\mathbf{r}' \rho(\mathbf{r}') \frac{\exp(ik_0 |\mathbf{r} - \mathbf{r}'|)}{k_0 |\mathbf{r} - \mathbf{r}'|} \tilde{\beta}(\mathbf{r}') = -(2\delta + i) \tilde{\beta}(\mathbf{r}) + e^{ik_0 \cdot \mathbf{r}}, \quad (2.4)$$

where we have introduced the normalized detuning $\delta = \Delta_0/\Gamma$ and the excitation field $\tilde{\beta}(\mathbf{r}) = (\hbar\Gamma/dE_0)\beta(\mathbf{r})$. Let us remark that the kernel of the integral of (2.4) is the Green function for the Helmholtz equation:

$$(\nabla^2 + k_0^2) \frac{\exp(ik_0 |\mathbf{r} - \mathbf{r}'|)}{|\mathbf{r} - \mathbf{r}'|} = -4\pi\delta(\mathbf{r} - \mathbf{r}') \quad (2.5)$$

and that $(\nabla^2 + k_0^2) \exp(ik_0 \cdot \mathbf{r}) = 0$. Then, applying $(\nabla^2 + k_0^2)$ to (2.4) we obtain that $\tilde{\beta}(\mathbf{r})$ satisfies the Helmholtz equation

$$[\nabla^2 + k_0^2 m_0^2(\mathbf{r})] \tilde{\beta}(\mathbf{r}) = 0, \quad (2.6)$$

where $m_0(\mathbf{r})$ is the local refraction index of the atomic cloud:

$$m_0^2(\mathbf{r}) = 1 - \frac{4\pi\rho(\mathbf{r})}{k_0^3(2\delta + i)}. \quad (2.7)$$

Hence, the field $\tilde{\beta}(\mathbf{r})$ propagates as a wave in the cloud of cold atoms, which acts as a ‘classical’ dielectric medium of the index $m_0(\mathbf{r})$. The imaginary part of m_0 originates in the single-atom decay term and is responsible for the diffusive nature of the cloud: it vanishes only in the limit of the far-detuned incident laser.

3. Scattered intensity and radiation pressure force

From the local response $\beta(\mathbf{r}, t)$ to the external field, many measurable quantities can be derived, such as the scattered intensity and the radiation pressure force (Courteille et al. 2010). The scattered field is (Bachelard et al. 2011)

$$E_s(\mathbf{r}, t) = -E_0 \int d\mathbf{r}' \rho(\mathbf{r}') \frac{\exp(ik_0 |\mathbf{r} - \mathbf{r}'|)}{k_0 |\mathbf{r} - \mathbf{r}'|} \tilde{\beta}(\mathbf{r}', t) \quad (3.1)$$

and the far-field scattered intensity, at distance r and direction (θ, ϕ) with respect to the z -axis, reads

$$I_s(r, \theta, \phi) = c\epsilon_0 \frac{E_0^2}{k_0^2 r^2} [N \langle |\tilde{\beta}(\mathbf{r})|^2 \rangle + N^2 |s(\mathbf{k})|^2], \quad (3.2)$$

where

$$\langle |\tilde{\beta}(\mathbf{r})|^2 \rangle = \frac{1}{N} \int d\mathbf{r}' \rho(\mathbf{r}') |\tilde{\beta}(\mathbf{r}')|^2 \quad (3.3)$$

and $s(\mathbf{k})$ is the structure factor,

$$s(\mathbf{k}) = \frac{1}{N} \int d\mathbf{r} \rho(\mathbf{r}) \tilde{\beta}(\mathbf{r}) e^{-i\mathbf{k} \cdot \mathbf{r}}, \quad (3.4)$$

with $\mathbf{k} = k_0(\sin \theta \cos \phi, \sin \theta \sin \phi, \cos \theta)$. The first term of (3.2) corresponds to the incoherent and isotropic contribution, and is proportional to N , whereas the second term is the superradiant, strongly directional, scattered intensity, and it is proportional to N^2 . Hence, the cooperation of an increasing number of atoms to scatter light leads to a more coherent and focused emission – superradiance dominates over single-atom scattering.

Another observable of interest is the radiation pressure force, that is the net force that the light exerts on the atoms. It is the sum of two contributions, the first due to absorption of photons from the incident field and the second one due to their spontaneous re-emission along any direction (θ, ϕ) (Courteille et al. 2010; Bachelard et al. 2011). The force on the cloud center of mass and along the z -axis reads

$$\langle F_z \rangle = \langle F_z^a \rangle + \langle F_z^e \rangle, \quad (3.5)$$

where

$$\langle F_z^a \rangle = -2\pi\epsilon_0 \frac{E_0^2}{k_0^2} \text{Im}(s(\mathbf{k}_0)), \quad (3.6)$$

$$\langle F_z^e \rangle = -\epsilon_0 \frac{E_0^2 N}{2k_0^2} \int d\Omega_k \cos \theta |s(\mathbf{k})|^2, \quad (3.7)$$

with $d\Omega_k = d\phi d\theta \sin \theta$ as the elementary solid angle. The absorption force \mathbf{F}^a is directed along the z -axis and it is proportional to the incident intensity, $I_0 = \epsilon_0 c E_0^2$,

since it corresponds to the absorption of laser photons. The emission force \mathbf{F}^e is directed along \mathbf{k} , and its z -component is obtained by averaging over the solid angle the product between the emission probability of the photons $|s(\mathbf{k})|^2$ and the projection of their momentum on the z -axis, hence the factor $\cos \theta$. The integration over the solid angle Ω_k in (3.7) is performed using the identity

$$\int d\Omega_k \cos \theta e^{i\mathbf{k} \cdot (\mathbf{r} - \mathbf{r}')} = 4\pi i \frac{z - z'}{|\mathbf{r} - \mathbf{r}'|} j_1(k_0|\mathbf{r} - \mathbf{r}'|) \\ = -\frac{4\pi i}{k_0} \frac{\partial}{\partial z} j_0(k_0|\mathbf{r} - \mathbf{r}'|), \quad (3.8)$$

where $j_0(x) = \sin(x)/x$ and $j_1(x) = \sin(x)/x^2 - \cos(x)/x$ are the zeroth and first-order spherical Bessel functions. Using (3.8), the emission force is written as

$$\langle F_z^e \rangle = 2\pi\epsilon_0 \frac{E_0^2}{k_0^2 N} \text{Re} \left[\int d\mathbf{r} \rho(\mathbf{r}) \tilde{\beta}^*(\mathbf{r}) \frac{\partial}{\partial z} \right. \\ \left. \times \int d\mathbf{r}' \rho(\mathbf{r}') \frac{\exp(ik_0|\mathbf{r} - \mathbf{r}'|)}{k_0|\mathbf{r} - \mathbf{r}'|} \tilde{\beta}(\mathbf{r}') \right]. \quad (3.9)$$

Combining (3.6) and (3.9) allows us to write the total force as

$$\langle F_z \rangle = \frac{1}{N} \int d\mathbf{r} \rho(\mathbf{r}) \text{Re} \left\{ -d\beta^*(\mathbf{r}) \nabla_z [E_0 e^{ik_0 \mathbf{r}} \right. \\ \left. - E_0 \int d\mathbf{r}' \rho(\mathbf{r}') \frac{\exp(ik_0|\mathbf{r} - \mathbf{r}'|)}{k_0|\mathbf{r} - \mathbf{r}'|} \tilde{\beta}(\mathbf{r}') \right\}. \quad (3.10)$$

Since the term in the square bracket is the total electric field $E_t(\mathbf{r}) = E_0 e^{ik_0 \mathbf{r}} + E_s(\mathbf{r})$, i.e. the sum of the incident and scattered field given by (3.1), the force on the center of mass appears as the average over the local force on the atoms:

$$\mathbf{F} = -d \text{Re}(\beta^* \nabla_r E_t). \quad (3.11)$$

Hence, we recover the well-known expression of the force that a light field exerts on an atom (Gordon and Ashkin 1980), though a crucial difference is that E_t here contains the self-radiated field of the cloud. Note also that in (3.11), we have extended our expression (3.10) to every spatial direction.

4. Mie scattering

As discussed before, the knowledge of the excitation probability $\beta(\mathbf{r})$ is the key to understanding the radiation pattern and the forces exerted on the atomic cloud. Despite the three-dimensional nature of the problem, an analytical solution exists for simple geometries. We here focus on clouds with spherical symmetry $\rho(r)$, for which the eigenmodes of the wave equation have the form $u_n(r)P_n(\cos \theta)$, with $P_n(x)$ as the n th Legendre polynomial and $u_n(r)$ a radial mode that satisfies (Bachelard et al. 2012b)

$$u_n''(r) + 2\frac{u_n'(r)}{r} + \left[k_0^2 m_0^2(r) - \frac{n(n+1)}{r^2} \right] u_n(r) = 0. \quad (4.1)$$

Because of the rotational symmetry, no dependence on ϕ is present. The excitation field is then decomposed as a sum of partial waves:

$$\tilde{\beta}(r, \theta) = \sum_{n=0}^{\infty} (2n+1) \beta_n u_n(r) P_n(\cos \theta), \quad (4.2)$$

whereas the incident wave is decomposed as

$$e^{ik_0 \mathbf{r}} = \sum_{n=0}^{\infty} i^n (2n+1) j_n(k_0 r) P_n(\cos \theta). \quad (4.3)$$

Finally, the scattering kernel is expanded in partial waves, using the identity

$$\frac{\exp(ik_0|\mathbf{r} - \mathbf{r}'|)}{k_0|\mathbf{r} - \mathbf{r}'|} = 4\pi i \sum_{n=0}^{\infty} \sum_{m=-n}^n Y_{n,m}(\hat{r}) Y_{n,m}^*(\hat{r}') \\ \times \begin{cases} j_n(k_0 r') h_n^{(1)}(k_0 r) & \text{for } r > r' \\ j_n(k_0 r) h_n^{(1)}(k_0 r') & \text{for } r < r' \end{cases} \quad (4.4)$$

where \hat{r} and \hat{r}' are unit vectors in the directions of \mathbf{r} and \mathbf{r}' , $Y_{n,m}$ is the spherical harmonics (in particular, $Y_{n,0}(\theta, \phi) = \sqrt{(2n+1)/4\pi} P_n(\cos \theta)$), and $j_n(z)$ and $h_n^{(1)}(z)$ are the spherical Bessel functions. Inserting (4.2)–(4.4) into (2.4) and projecting on the orthogonal basis of the Legendre polynomial, we obtain the relation

$$j_n(k_0 r) = (2\delta + i) \beta_n u_n(r) + \beta_n f_n(r), \quad (4.5)$$

where

$$f_n(r) = 4\pi i \int_0^{\infty} dr' r'^2 \rho(r') u_n(r') \\ \times \begin{cases} j_n(k_0 r') h_n^{(1)}(k_0 r) & \text{for } r > r' \\ j_n(k_0 r) h_n^{(1)}(k_0 r') & \text{for } r < r' \end{cases}. \quad (4.6)$$

Once specified the form for $\rho(r)$, the solution for the radial mode u_n can be derived, and the amplitude of each partial wave β_n calculated from (4.5) and (4.6). Assuming a finite cloud of radius R , such that $\rho(r) = 0$ for $r > R$, it reads (Bachelard et al. 2012b)

$$\beta_n = \frac{j_n(k_0 R)}{(2\delta + i) u_n(R) + i \lambda_n h_n^{(1)}(k_0 R)} \quad (4.7)$$

with

$$\lambda_n = 4\pi \int_0^{\infty} dr r^2 \rho(r) j_n(k_0 r) u_n(r), \quad (4.8)$$

and where we have used that

$$f_n(R) = 4\pi i h_n^{(1)}(k_0 R) \int_0^R dr' r'^2 \rho(r') u_n(r') j_n(k_0 r') \\ = i \lambda_n h_n^{(1)}(k_0 R). \quad (4.9)$$

The cloud structure factor is then easily derived (Bachelard et al. 2011):

$$s(\mathbf{k}) = \frac{1}{N} \sum_{n=0}^{\infty} (2n+1) \lambda_n \beta_n P_n(\cos \theta), \quad (4.10)$$

as well as the isotropic radiation contribution:

$$\langle |\tilde{\beta}(\mathbf{r})|^2 \rangle = \frac{1}{N} \sum_{n=0}^{\infty} (2n+1) \tilde{\lambda}_n |\beta_n|^2, \quad (4.11)$$

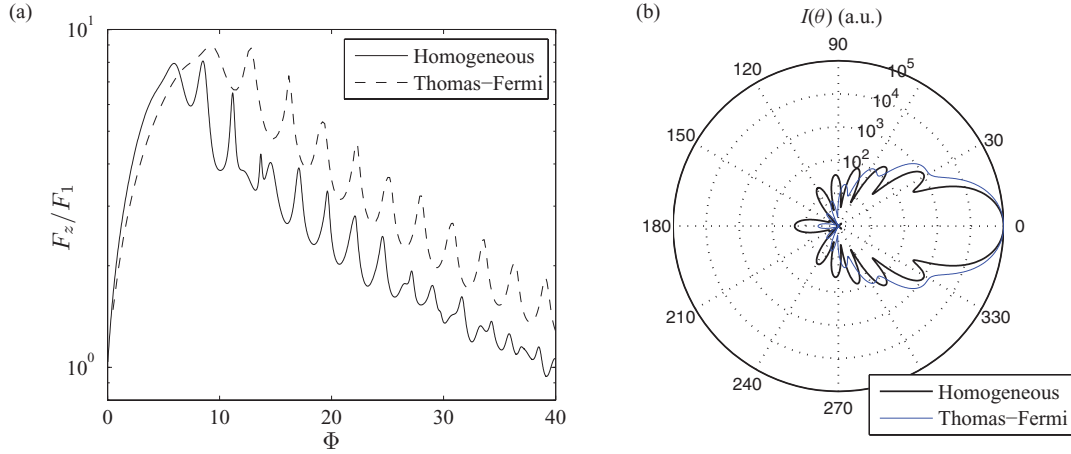


Figure 1. (Colour online) (a) Radiation pressure force as a function of the phase-shift Φ for homogeneous (plain line) and Thomas-Fermi (dashed line) distributions. Simulations realized for a cloud of size $k_0 R = 10$, a detuning $\delta = -50$ and varying the number of atoms N . The force is normalized by the single atom force $F_1 = 2\pi\epsilon_0(E_0/k_0)^2/(1+4\delta^2)$, which is observed in the absence of collective effects. (b) Radiation pattern $I(\theta)$ for homogeneous (thick black line) and Thomas-Fermi (blue thin line) distributions. Simulations realized for a cloud of size $k_0 R = 10$, detuning $\delta = -50$ and $N = 6100$ atoms.

where

$$\tilde{\lambda}_n = 4\pi \int_0^\infty dr r^2 \rho(r) |u_n(r)|^2. \quad (4.12)$$

The problem of scattering by a homogeneous spherical dielectrics was initially investigated by Mie (1908), and it was later generalized to homogeneous ellipsoids. In the case of a homogeneous spherical atomic cloud of N atoms and radius R , the index is $m_0 = \sqrt{1 - 3N/(k_0 R)^3(2\delta + i)}$, and the radial solution of the Helmholtz equation is $u_n(r) = j_n(m_0 k_0 r)$. Using the special properties of the Bessel functions, λ_n is explicitly calculated:

$$\lambda_n = (2\delta + i)(k_0 R)^2 [m_0 j_{n-1}(m_0 k_0 R) j_n(k_0 R) - j_{n-1}(k_0 R) j_n(m_0 k_0 R)], \quad (4.13)$$

and the complex amplitude of the n th partial wave is deduced:

$$\beta_n = \frac{j_n(k_0 R)}{(2\delta + i)j_n(m_0 k_0 R) + i\lambda_n h^{(1)}(k_0 R)}. \quad (4.14)$$

As can be observed in Fig. 1, when the optical density is tuned – here varying the number of particles at fixed volume and detuning, the force that pushes the cloud exhibits some oscillations. These resonances correspond to the cloud acting as a resonant cavity for the light, and are best understood by introducing the phase-shift experienced by the light inside the cloud: $\Phi = \int (m_0(0,0,z) - 1)dz$. When this phase-shift is a multiple of π , the cavity that the cloud forms is at resonance with the light, so a greater amount of light is stored in the atomic cloud and the radiation pressure force increases (Bachelard et al. 2012b).

Yet the spiky structure of the force for homogeneous clouds hides more complex resonances. It is known that the sharp index interface between a dielectric and, say, vacuum allows for surface modes to propagate. These are called whispering gallery modes (Nussenzveig

1992). They are characterized by sharp resonances whose number, positions and amplitudes strongly depend on the cloud characteristics, making them a powerful tool to characterize the scatterers (Oraevsky 2002).

This exact solution of the scattering problem as an infinite series of partial waves is reminiscent of the Mie solution (Mie 1908; van de Hulst 1981), although our approach is slightly different: Mie used continuity equations for the tangential field components at the dielectric boundary, while we adopted an integral formulation of the problem. The two solutions are nevertheless formally the same (Bachelard et al. 2012b), as far as finite clouds are concerned. Let us also remark that our solution is more general, since it holds for any radial solution $u_n(r)$ of the Helmholtz equation, i.e. it applies to any spherical cloud with arbitrary density. It is thus of particular interest for atomic clouds where the traps in general generate inhomogeneous density profiles.

5. Ultra-cold clouds

Ultra-cold clouds of fermionic species have been successfully described by quadratic profiles of density, following the pioneering work of Llewellyn Thomas and Enrico Fermi on distributions of electrons (Fermi 1927; Thomas 1927). These clouds exhibit a parabolic density $\rho(r) = (5N/2V)[1 - r^2/R^2]$, with R being the radius of the cloud and $V = 4\pi R^3/3$ its volume, and consequently a spatially dependent refraction index:

$$m_0^2(r) = m_c^2 + \gamma^2 r^2, \quad (5.1)$$

with $m_c = \sqrt{1 - (15/2)N/(k_0 R)^3(2\delta + i)}$ as the index in the core of the sample, and $\gamma^2 = (15/2)N/(k_0^3 R^5)(2\delta + i)$. Using the substitution $u_n(r) = r^{-3/2}w_n(x)$, with $x = \gamma r^2/2$, one can show that $w_n(x)$ satisfies the Coulomb wave equation, well known in nuclear physics (Martin 2002), whose solutions are the Coulomb wave functions $w_n(x) = F_{n/2-1/4}(-m_c^2/4\gamma, x)$. We get the following

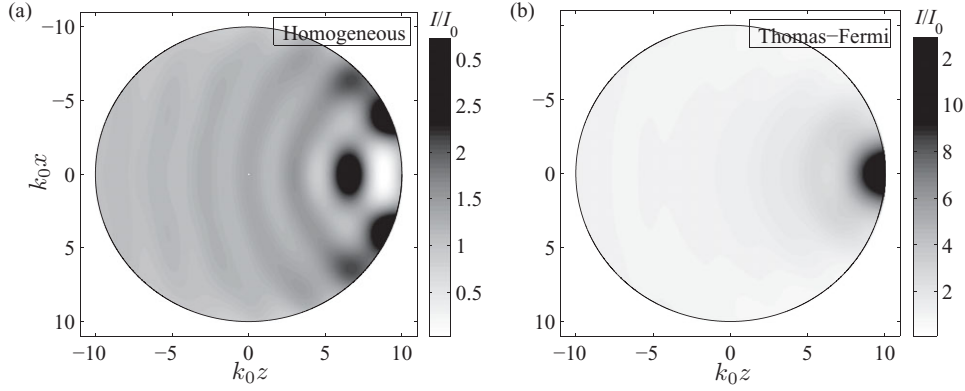


Figure 2. Light intensity in the cloud with homogeneous (a) and Thomas–Fermi (b) distributions, in the plane $y = 0$. Simulations realized for a cloud of size $k_0 R = 10$, a detuning $\delta = -50$ and $N = 6100$ atoms. The intensity is normalized to the laser intensity I_0 .

partial wave expansion for the excitation field:

$$\tilde{\beta}(r, \theta) = \sum_{n=0}^{\infty} (2n+1) \frac{\beta_n}{r^{3/2}} F_{\frac{n}{2}-\frac{1}{4}} \left(-\frac{m_c^2}{4\gamma}, \frac{\gamma r^2}{2} \right) P_n(\cos \theta). \quad (5.2)$$

Apart from the fact that studying the scattering by atomic clouds with a quadratic density rather than a homogeneous one is a much more realistic approximation, the former profile also yields different physics. Indeed, as can be observed in Fig. 1, the spiky structure of the whispering gallery modes disappears, and only the regular oscillations of the longitudinal cavity modes, such that the longitudinal phase-shift in the cloud is a multiple of π , survive. Indeed, because the change in the refractive index is much smoother in clouds with a Thomas–Fermi distribution than with a homogeneous one, the surface modes cannot propagate anymore.

This analysis is confirmed by the profiles of light intensity in the cloud (see Fig. 2). One can observe that homogeneous spheres exhibit off-axis surface modes (Fig. 2a) – this feature was checked for various sets of parameters. These surface modes create new resonances that compete with the longitudinal ones, causing the spiky structure observed in Fig. 1 for the center-of-mass force. These off-axis modes appear much weaker in clouds with the Thomas–Fermi distribution (Fig. 2b).

6. Thermal clouds

Finally, we discuss the Mie scattering solution in clouds with boundaries extending until $r = \infty$. For instance, thermal clouds with a Maxwell–Boltzmann velocity distribution have a Gaussian density profile, so the Mie scattering solution that makes use of finite boundary conditions cannot be used straightforwardly. Here, we propose an alternative derivation that holds as well for such distributions with boundaries at infinite. To our knowledge, it is the first solution to the Mie scattering problem with infinite boundaries.

Starting from (4.5), the amplitude β_n of the n th partial wave can be obtained by multiplying both terms

by $4\pi r^2 \rho(r) j_n(k_0 r)$ and integrating over r :

$$\beta_n = \frac{A_n}{(2\delta + i)\lambda_n + B_n}, \quad (6.1)$$

where we have introduced:

$$A_n = 4\pi \int_0^\infty dr r^2 \rho(r) j_n^2(k_0 r), \quad (6.2)$$

$$B_n = 4\pi \int_0^\infty dr r^2 \rho(r) j_n(k_0 r) f_n(r). \quad (6.3)$$

Using (4.6), the coefficient B_n can be written as

$$B_n = 16\pi^2 i \int_0^\infty dr r^2 \rho(r) j_n(k_0 r) \times \left\{ h_n^{(1)}(k_0 r) \int_0^r dr' r'^2 \rho(r') u_n(r') j_n(k_0 r') + j_n(k_0 r) \int_r^\infty dr' r'^2 \rho(r') u_n(r') h_n^{(1)}(k_0 r') \right\}. \quad (6.4)$$

Using the identities (A 5) and (A 6) of Appendix, and the identity $j_n(z) h_n^{(1)'}(z) - h_n^{(1)}(z) j_n'(z) = i/z^2$, one can show that

$$B_n = (2\delta + i)(-\lambda_n + iA_n D_n) \quad (6.5)$$

with

$$D_n = \lim_{r \rightarrow \infty} \left\{ r^2 \left[h_n^{(1)}(k_0 r) u_n(r) - u_n(r) h_n^{(1)'}(k_0 r) \right] \right\}. \quad (6.6)$$

One deduces that

$$\beta_n = \frac{1}{i(2\delta + i)D_n} = \frac{1}{2\delta + i} \lim_{r \rightarrow \infty} \left\{ \frac{1}{ir^2 \left[h_n^{(1)}(k_0 r) u_n'(r) - u_n(r) h_n^{(1)'}(k_0 r) \right]} \right\}. \quad (6.7)$$

As for the eigenvalues λ_n of the scattering problem, they read

$$\lambda_n = 4\pi \int_0^\infty dr r^2 \rho(r) j_n(k_0 r) u_n(r) = (2\delta + i) \times \lim_{r \rightarrow \infty} \left\{ r^2 [j_n(k_0 r) u_n'(r) - u_n(r) j_n'(k_0 r)] \right\}. \quad (6.8)$$

Thus, the scattering coefficients are determined by the value of the radial modes $u_n(r)$ and of their first derivative at $r \rightarrow \infty$.

7. Discussion

Here, we have discussed the light scattering by a macroscopic atomic cloud, when the atoms cooperate to scatter the light superradiantly. The cloud was considered as a fluid, i.e. the point-like nature of the microscopic scatterers was neglected, and an analytical solution was then derived for spherical geometries, where the excitation field inside the cloud is developed as the sum of partial waves. Although we generalized it to arbitrary spherical densities, this technique is formally equivalent to Mie scattering, where continuity equations are used at the boundaries of the scattering medium. Furthermore, our technique allowed for the derivation of a solution to the Mie problem for clouds with infinite boundaries. An accurate treatment of the decay of the density profile is crucial to understand if some special resonances, such as whispering gallery modes, may exist or not. It is also important in the context of atomic clouds or plasmas where, different from solid dielectrics, the densities are usually strongly non-homogeneous.

Appendix. Integral identities for the radial eigenmodes $u_n(r)$

The function $u_n(r)$ is a solution of the differential equation (4.1):

$$u_n'' + 2\frac{u_n'}{r} + \left[k_0^2 m_0^2(r) - \frac{n(n+1)}{r^2} \right] u_n = 0, \quad (\text{A } 1)$$

where $m_0^2(r) = 1 - 4\pi\rho(r)/k_0^3(2\delta + i)$. Defining $v_n(r) = ru_n(r)$, (A 1) becomes

$$v_n'' + \left[k_0^2 m_0^2(r) - \frac{n(n+1)}{r^2} \right] v_n = 0. \quad (\text{A } 2)$$

For $m_0(r) = 1$, the solution is $q_n(r) = rj_n(k_0r)$. Introducing $P(r) = k_0^2 m_0^2(r) - n(n+1)/r^2$ and $Q(r) = k_0^2 - n(n+1)/r^2$, we get $v_n'' + P v_n = 0$ and $q_n'' + Q q_n = 0$, so that

$$\int dr (Q - P) v_n q_n = q_n v_n' - v_n q_n'. \quad (\text{A } 3)$$

Since

$$(Q - P) v_n q_n = k_0^2 (1 - m_0^2) v_n q_n = \frac{4\pi\rho(r)}{k_0(2\delta + i)} r^2 u_n(r) j_n(k_0r), \quad (\text{A } 4)$$

we obtain the indefinite integral

$$\begin{aligned} & \frac{4\pi}{k_0} \int^r dr' r'^2 \rho(r') u_n(r') j_n(k_0r') \\ &= (2\delta + i) r^2 \{ j_n(k_0r) u_n'(r) - u_n(r) j_n'(k_0r) \}. \end{aligned} \quad (\text{A } 5)$$

In a similar way, we obtain

$$\begin{aligned} & \frac{4\pi}{k_0} \int^r dr' r'^2 \rho(r') u_n(r') h_n^{(1)}(k_0r') \\ &= (2\delta + i) r^2 \{ h_n^{(1)}(k_0r) u_n'(r) - u_n(r) h_n^{(1)'}(k_0r) \}. \end{aligned} \quad (\text{A } 6)$$

References

- Bachelard, R., Bender, H., Courteille, Ph. W., Piovella, N., Stehle, C., Zimmermann, C. and Slama, S. 2012a The role of Mie scattering in the seeding of matter-wave superradiance. *Phys. Rev. A* **86**, 043605.
- Bachelard, R., Courteille, Ph. W., Kaiser, R. and Piovella, N. 2012b Resonances in Mie scattering by an inhomogeneous atomic cloud. *EPL* **97**, 14 004.
- Bachelard, R., Piovella, N. and Courteille, Ph. W. 2011 Cooperative scattering and radiation pressure force in dense atomic clouds. *Phys. Rev. A* **84**, 013821.
- Bender, H., Stehle, C., Slama, S., Kaiser, R., Piovella, N., Zimmermann, C. and Courteille, Ph. W. 2010 Observation of cooperative Mie scattering from an ultracold atomic cloud. *Phys. Rev. A* **82**, 011404.
- Bienaimé, T., Bux, S., Lucioni, E., Courteille, Ph. W., Piovella, N. and Kaiser, R. 2010 Observation of cooperative radiation pressure in presence of disorder. *Phys. Rev. Lett.* **104**, 183602.
- Courteille, Ph. W., Bux, S., Lucioni, E., Lauber, K., Bienaimé, T., Kaiser, R. and Piovella, N. 2010 Modification of radiation pressure due to cooperative scattering of light. *Eur. J. Phys. D* **58**, 69.
- Fermi, E. 1927 Un metodo statistico per la determinazione di alcune proprietà dell'atomo. *Rend. Accad. Naz. Lincei* **6**, 602–607.
- Friedberg, R., Hartman, S. R. and Manassah, J. T. 1973 Frequency shifts in emission and absorption by resonant systems of two-level atoms. *Phys. Rep.* **7**, 101.
- Gordon, J. P. and Ashkin, A. 1980 Motion of atoms in a radiation trap. *Phys. Rev. A* **21**, 1980.
- Martin, P. A. 2002 Acoustic scattering by inhomogeneous spheres. *J. Acoust. Soc. Am.* **111**, 2013.
- Mendonça, J. T., Kaiser, R., Terças, H. and Loureiro, J. 2008 Collective oscillations in ultracold atomic gas. *Phys. Rev. A* **78**, 013408.
- Mendonça, J. T. and Terças, H. 2013 Physics of ultra-cold matter. In: *Springer Series on Atomic, Optical, and Plasma Physics*, Vol. 70. Springer, Berlin.
- Mie, G. 1908 Beiträge zur optik trüber medien, speziell kolloidaler metallösungen. *Ann. Phys.* **330**, 377.
- Nussenzweig, H. M. 1992 *Diffraction Effects in Semiclassical Scattering*. Cambridge University Press, Cambridge UK.
- Oraevsky, A. N. 2002 Acoustic scattering by inhomogeneous spheres. *Quantum. Electron.* **32**, 377.
- Prasad, S. and Glauber, R. J. 2010 Coherent radiation by a spherical medium of resonant atoms. *Phys. Rev. A* **82**, 063805.
- Scully, M. O., Fry, E. S., Ooi, C. H. R. and Wodkiewicz, K. 2006 Directed spontaneous emission from an extended ensemble of n atoms: timing is everything. *Phys. Rev. Lett.* **96**, 010501.

- Scully, M. O. and Svidzinsky, A. A. 2009 The effects of the n atom collective lamb shift on single photon superradiance. *Phys. Lett. A* **373**, 1283.
- Scully, M. O. and Svidzinsky, A. A. 2010 The lamb shift – yesterday, today, and tomorrow. *Science* **328**, 1239.
- Svidzinsky, A. A., Chang, J. T. and Scully, M. O. 2008 Dynamical evolution of correlated spontaneous emission of a single photon from a uniformly excited cloud of n atoms. *Phys. Rev. Lett.* **100**, 160504.
- Svidzinsky, A. A., Chang, J.-T. and Scully, M. O. 2010 Cooperative spontaneous emission of n atoms: many-body eigenstates, the effect of virtual lamb shift processes, and analogy with radiation of n classical oscillators. *Phys. Rev. A* **81**, 053821.
- Thomas, L. H. 1927 The calculation of atomic fields. *Proc. Cambridge Phil. Soc.* **23**, 542–548.
- van de Hulst, H. C. 1981 *Light Scattering by Small Particles*. Dover, New York, USA.